Research on Chemical Intermediates
https://doi.org/10.1007/s11164-020-04287-5

Preparation of thiazolidin-4-one derivatives using ZnO–NiO–$NiFe_2O_4$ nano-composite system

Mojtaba Lashkari[1] · **Majid Ghashang**[2]

Received: 25 July 2020 / Accepted: 26 September 2020

Abstract

The hydrothermal synthesis of ZnO–NiO–$NiFe_2O_4$ nano-composite is reported. The sample was utilized to characterize via XRD, FE-SEM, EDS, FT-IR, UV–Vis, and BET techniques. The sample consisted of three different phases as ZnO (hexagonal), NiO (cubic), and $NiFe_2O_4$ (cubic) with the average particle size as 34 nm and specific surface area, average pore diameter, and pore volume as 64.35 $m^2\ g^{-1}$, 13.02 nm, and 0.201 $cm^3\ g^{-1}$, respectively. Catalytic behavior of the nano-composite was investigated on the synthesis of thiazolidin-4-one derivatives under thermal and ultrasonic irradiation condition. Our results show that the catalytic activity of ZnO–NiO–$NiFe_2O_4$ nano-composite is much higher than ZnO, NiO, and $NiFe_2O_4$ metal oxides. All products were prepared in high yields with short reaction times. In addition, the catalyst was recovered for at least five times.

Keywords Thiazolidin-4-one · 2-Methyl-5-(4-oxo-2-phenylthiazolidin-3-yl) thieno[3,4-d]pyrimidin-4(3H)-one · ZnO–NiO–$NiFe_2O_4$ nano-composite · Hydrothermal synthesis · $NiFe_2O_4$

Introduction

Heterocyclic scaffolds with N and S heteroatoms have fascinated chemists not only for the wide variety in their structure but also for their wide array of biological properties. As an example, thiazolidinones and thieno[3,4-*d*]pyrimidine derivatives are known as building blocks in drug design and synthesis and possess various

---

Electronic supplementary material The online version of this article (https://doi.org/10.1007/s11164-020-04287-5) contains supplementary material, which is available to authorized users.

✉ Mojtaba Lashkari
mojtaba_chem_84@yahoo.com; m.lashkari@velayat.ac.ir

[1] Faculty of Sciences, Velayat University, P.O. Box 9911131311, Iranshahr, Iran

[2] Department of Chemistry, Najafabad Branch, Islamic Azad University, P.O. Box 517, Najafabad, Iran

pharmacological activities [1–4]. The widespread use of structures containing thiazolidine nuclei has led scientists to pay special attention to develop the synthesis and design of chemical structures with thiazolidine nuclei, and for this reason, a number of methods have been developed for the synthesis of diverse thiazolidine derivatives. Among these reported protocols, those that use the multi-component reaction of aldehydes, amines, and thioglycolic acid are simple and more favorable due to the structure diversity, easy to work, and product purification [5–13].

On the other hand, metal oxides are a good choice for use as a catalyst in many chemical reactions due to their thermal and chemical stability and attracted the attention of chemists for many years. Although metal oxides are useful and applicable materials, the improvement in their characteristics in many cases is necessary [14, 15]. One way is to make a composite of metal oxides. Composites usually retain or strengthen the properties of their components. For example, our findings have been shown that ZnO-based nano-composites could be used as a more effective catalyst in organic transformations than ZnO alone [16–18]. In particular, composites of metal oxides have been found to be more suitable materials for use in transportation industries, lighting and electronics, photometry, and catalytic applications. In addition, composites have improved properties compared to single-metal oxides [15]. From another view of point, the composites of transition metal ferrites are promising catalysts for a variety of chemical reactions such as decolorization of an azo dye, synthesis of amides, partial oxidation of C_3H_6 to surface carboxylates and NO oxidation to NO_2, synthesis of bis(dihydropyrimidinone)benzene and 3,4-dihydropyrimidin-2(1*H*)-ones, and vapor phase oxidation of benzoic acid to phenol [19–23]. Magnetic composites are more advantageous compared to non-magnetic materials as these materials are due to their structural, electronic, high catalytic potentials, and ease of recovery [24–27]. Thus, the use of metal oxides magnetic composites could be associated with the environmental and economic impacts.

In the present work, we plan to fabricate $ZnO–NiO–NiFe_2O_4$ nano-composite through a simple hydrothermal synthetic method and evaluation of its catalytic potential on the preparation of thiazolidin-4-one derivatives.

Experimental section

Preparation of $ZnO–NiO–NiFe_2O_4$ nano-composite

ZnO nano-powders were prepared according to our previous report [28].

In a 250-mL beaker, ZnO nano-powders (1.0 mmol) were dispersed in a 25 mL aqueous solution of $FeCl_3·6H_2O$ (2.0 mmol) and $NiSO_4·6H_2O$ (2.0 mmol) by ultrasonic technique for 60 min. Next, a solution of NaOH (10%) was added dropwise until the pH = 12. The mixture was sonicated for 60 min and subsequently was transferred into an autoclave oven (100 mL) and kept at 200 °C for 24 h. Finally, the prepared $ZnO–NiO–NiFe_2O_4$ nano-composite was filtered and washed with water and dried at 100 °C.

General procedure for the preparation of thiazolidin-4-one derivatives

To a mixture of amine (**1/5**, 1.0 mmol), aldehyde (**2/6**, 1.0 mmol), and thioglycolic acid (**3**, 1.0 mmol) in DMF (10 mL) was added ZnO–NiO–$NiFe_2O_4$ nano-composite (0.025 g), and the mixture was refluxed (or sonicated at 100 °C) until the reaction was completed (TLC monitoring). At last, the solvent was concentrated under reduced pressure and the reaction mixture was purified using plate chromatography (silica plates, n-hexane/ethyl acetate 3/1).

Results and discussion

The XRD pattern was used to determine the crystallinity of the ZnO–NiO–$NiFe_2O_4$ nano-composite. The XRD pattern shows three phases as ZnO (hexagonal, JCPDS PDF No. 00-036-1451) with the distinctive peaks as 31.8, 34.4, 36.2, 47.5, 56.6, 62.9, 67.9, and 69.1 [2θ°], NiO (cubic, JCPDS PDF No. 00-002-1239) with the following distinctive peaks as 37.4, 43.4, 62.2, 75.4, and 79.9 [2θ°], and $NiFe_2O_4$ (cubic, JCPDS PDF No. 00-010-0325) designed with the following peaks as 18.4, 30.3, 35.7, 43.4, 57.3, 62.9, and 74.6 [2θ°] without any other phases or impurities (Fig. 1). The FE-SEM image shows the shapeless morphology of the particles and shows the uniform distribution of the phases involved in the composite mixture. The average particle size was determined by the particle size distribution analysis by the DLS technique, and the results showed that the sample consists of particles of less than 100 nm in size ZnO–NiO–$NiFe_2O_4$. The average particle size determined by this method was 34 nm. The results of EDS analysis confirm the presence of Zn, Ni, and Fe elements, and based on the molar ratio of the elements the chemical structure of nano-composite can be suggested as ZnO–NiO–$NiFe_2O_4$ (Fig. 2).

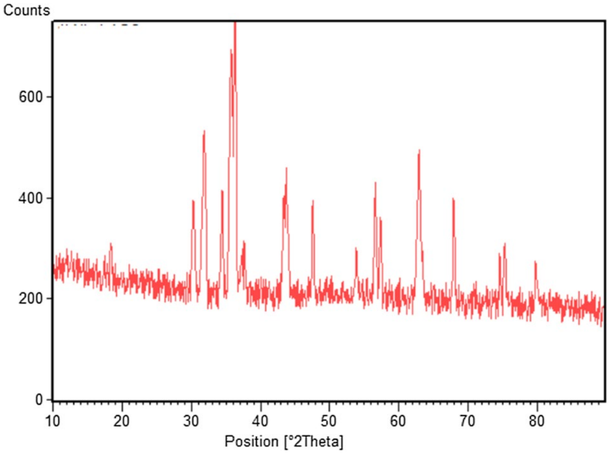

Fig. 1 XRD pattern of ZnO–NiO–$NiFe_2O_4$ nano-composite

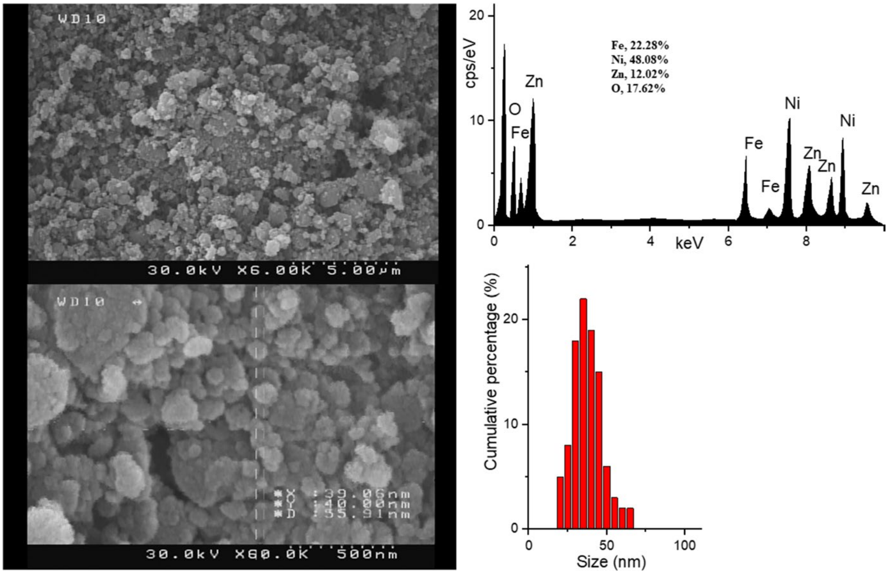

Fig. 2 FE-SEM, EDS, and DLS analysis of ZnO–NiO–$NiFe_2O_4$ nano-composite

The FT-IR analysis of ZnO–NiO–$NiFe_2O_4$ nano-composite is depicted in Fig. 3. The sharp signals below 700 cm^{-1} could be assigned to the stretching vibration of metal–oxygen bonds. The stretching vibration of the $Fe_2O_4^{2-}$ group is seen as a broad peak at about 1500 cm^{-1}. The broad peak located at 3300–3700 cm^{-1} is related to the stretching vibration of the O–H bond from the adsorbed water on the KBr disk. At the UV–visible absorption spectra, we found that ZnO–NiO–$NiFe_2O_4$ nano-composite discloses absorption at the UV region (Fig. 3). The noticed absorption peak centered at about 370 nm is due to the existence of the ZnO and NiO phases in a composite structure of them. The $NiFe_2O_4$ phase shows a lower intensity absorption peak at about 308 nm.

In order to characterize the surface area and possible porosity of ZnO–NiO–$NiFe_2O_4$ nano-composite, nitrogen adsorption–desorption analysis was used. Figure 3 shows the type IV of isotherm model with an H3-type hysteresis loop (IUPAC classification) that shows the mesoporous structure of the material. The physicochemical parameters of ZnO–NiO–$NiFe_2O_4$ nano-composite including specific surface area, average pore diameter, and pore volume were measured by the BET method as 64.35 $m^2\ g^{-1}$, 13.02 nm, and 0.201 $cm^3\ g^{-1}$, respectively [29, 30].

Synthesis of thiazolidin-4-one derivatives

At first, the reaction of 5-amino-2-methylthieno[3,4-d]pyrimidin-4(3H)-one (1.0 mmol), benzaldehyde (1.0 mmol), and thioglycolic acid (1.0 mmol) was chosen as the model to observe the effect of various solvents (H_2O, EtOH, EtOAc, hexane, Et_2O, DMF, and solvent-free condition), catalyst concentrations

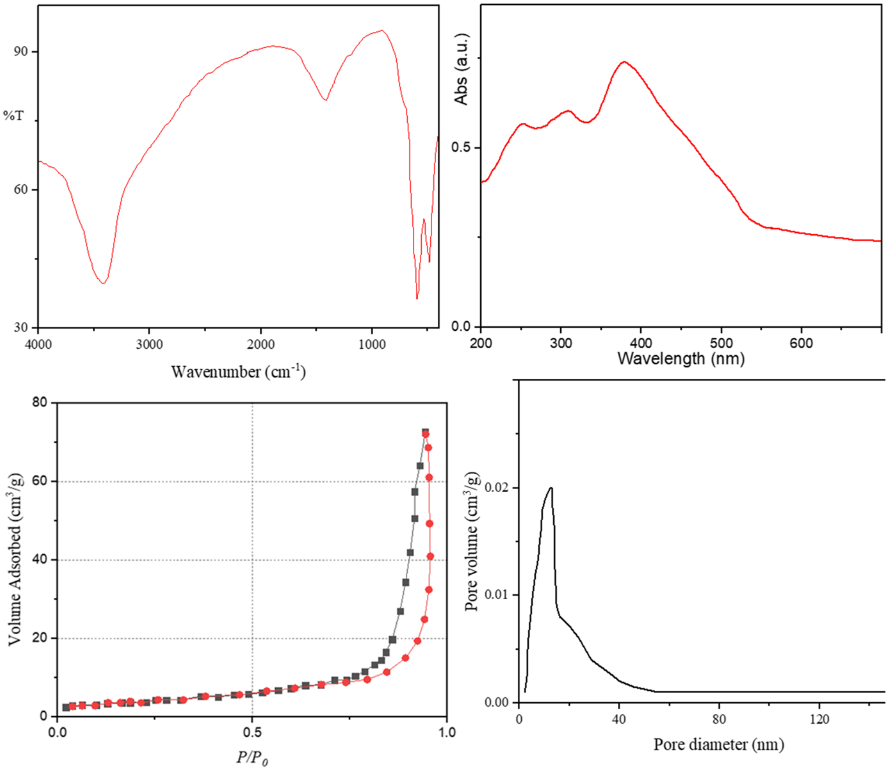

Fig. 3 FT-IR, UV–Vis, N_2 adsorption–desorption isotherm, and pore size distribution analysis of ZnO–NiO–$NiFe_2O_4$ nano-composite

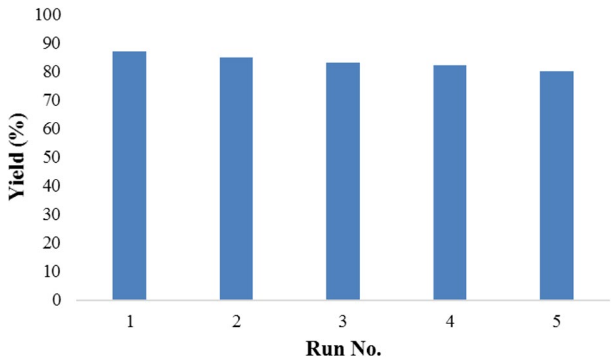

Fig. 4 Reusability of ZnO–NiO–$NiFe_2O_4$ nano-composite (preparation of **7a** using method A)

(0.01–0.1 g), and different metal oxides screening (ZnO, NiO, MgO, Fe_2O_3, Al_2O_3, CaO, Bi_2O_3, and $NiFe_2O_4$) on the product yield. The results are depicted in Table 1. The product (**4a**) was formed in low yields in solvents such as EtOH and EtOAc and in moderate yield under solvent-free condition, while solvents

Table 1 Optimization of the reaction conditions (based on the preparation of 2-methyl-5-(4-oxo-2-phenylthiazolidin-3-yl)thieno[3,4-d]pyrimidin-4(3H)-one (**4a**))

Entry	Catalyst (g)	Condition	Time (h)	Yield[a] (%)
1	0.025	H_2O, Reflux	8	–
2	0.025	EtOH, Reflux	8	35
3	0.025	EtOAc, Reflux	8	41
4	0.025	Hexane, Reflux	8	–
5	0.025	Et_2O, Reflux	8	–
6	**0.025**	**DMF, Reflux**	**3**	**95**
7	0.01	DMF, Reflux	8	32
8	0.05	DMF, Reflux	3	80
9	0.075	DMF, Reflux	2.5	83
10	0.1	DMF, Reflux	2.5	82
11	0.025	Solvent-free, 100 °C	3	65
12	**0.025**	**US, DMF, 100 °C**	**3**	**97**
13	ZnO (0.025 g)	DMF, Reflux	3	80
14	NiO (0.025 g)	DMF, Reflux	3	75
15	MgO (0.025 g)	DMF, Reflux	3	25
16	Fe_2O_3 (0.025 g)	DMF, Reflux	3	–
17	Al_2O_3 (0.025 g)	DMF, Reflux	3	–
18	CaO (0.025 g)	DMF, Reflux	3	–
19	Bi_2O_3 (0.025 g)	DMF, Reflux	3	–
20	$NiFe_2O_4$ (0.025 g)	DMF, Reflux	3	41

[a] Yields refer to the isolated product

Bold values indicate the optimized conditions

such as H_2O, hexane, and Et_2O are not suitable media for the preparation of the targeted compounds. Surprisingly, excellent yield (95%) of (**4a**) was obtained in dimethylformamide (DMF) as a solvent and using 0.025 g of ZnO–NiO–$NiFe_2O_4$ nano-composite as a catalyst. According to the results depicted in Table 1, higher dosages of the catalyst do not lead to a better yield of product (**4a**), whereas lower catalyst dosage resulted in poor yield (32%). Among the metal oxides screened, ZnO–NiO–$NiFe_2O_4$ nano-composite has distinctive better results. The synthesis of (**1d**) was done successfully under ultrasonic radiation conditions, and a high yield of product (97%) was obtained.

After optimization of the reaction condition, the scope and limitations for the preparation of products **4a–l** using other aromatic aldehydes were investigated (Scheme 1, Table 2). As shown in Table 2, all products were synthesized in high yields under short reaction times. The reaction of both aldehydes bearing electron-donating and electron-withdrawing groups results in high yields. However, electron-withdrawing groups have longer reaction times than those of electron-donating groups. The generality of the method was also examined under ultrasonic irradiation condition. As can be seen from Table 2, all target products were synthesized in excellent yields.

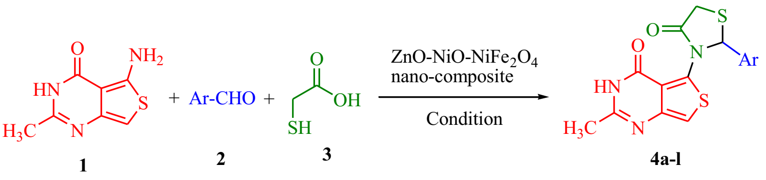

Scheme 1 Preparation of 2-methyl-5-(4-oxo-2-arylthiazolidin-3-yl)thieno[3,4-d]pyrimidin-4-(3*H*)-one derivatives (**4a–l**) using ZnO–NiO–$NiFe_2O_4$ nano-composite

Table 2 Preparation of thiazolidin-4-one derivatives (**4a–l**) using ZnO–NiO–$NiFe_2O_4$ nano-composite

Entry	Ar	Product	Method A time (h)/Yield (%)	Method B Time (h)/Yield (%)	Melting point (°C)
1	Ph	**4a**	3/95	3/97	120–122
2	4-$MeOC_6H_4$	**4b**	2.5/90	2.5/96	151–153
3	2-MeC_6H_4	**4c**	3/83	3/88	137–139
4	4-MeC_6H_4	**4d**	2.5/87	2.5/90	144–146
5	2-ClC_6H_4	**4e**	4/69	4/79	171–173
6	4-ClC_6H_4	**4f**	3.5/79	3.5/93	189–191
7	4-BrC_6H_4	**4g**	4/98	4/90	197–199
8	3-ClC_6H_4	**4h**	2.5/84	3/93	192–194
9	4-$(CH_3)_3CC_6H_4$	**4i**	2.5/94	2.5/91	188–190
10	3,4-$(CH_3O)_2C_6H_4$	**4j**	2.5/88	2.5/89	211–213
11	3,4,5-$(CH_3O)_3C_6H_4$	**4k**	2.5/90	2.5/88	203–205
12	4-$NO_2C_6H_4$	**4l**	5/78	5/77	190–192

Method A: DMF, reflux; Method B: US, DMF, 100 °C

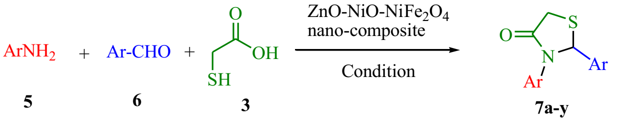

Scheme 2 Preparation of thiazolidin-4-one derivatives (**7a–y**) using ZnO–NiO–$NiFe_2O_4$ nano-composite

The method can be extended by the use of different amines. In continue, 5-amino-2-methylthieno[3,4-*d*]pyrimidin-4(3*H*)-one was replaced by different aromatic amines and the potential of ZnO–NiO–$NiFe_2O_4$ nano-composite was investigated as a catalyst on the three-component reaction of aromatic amines, aldehydes, and thioglycolic acid (Scheme 2). Different aromatic amines were successfully used in the reaction, and the corresponding products **(7a–y)** were obtained in high yields. The results are shown in Table 3. In general, electron-donating groups substituted on aromatic rings both in amines and in aldehydes have a positive effect on the reaction rate. Electron-donating groups such as methyl and methoxy increase the rate of the reaction, while electron-withdrawing groups decrease the rate of the reaction.

Table 3 Preparation of thiazolidin-4-one derivatives (**7a–y**) using ZnO–NiO–$NiFe_2O_4$ nano-composite

Entry	ArCHO	$ArNH_2$	Product	Method A Time (h)/Yield (%)	Method B Time (h)/Yield (%)
1	Ph	Ph	**7a**	2/87	2/91
2	4-MeC_6H_4	Ph	**7b**	1.8/90	1.8/93
3	3-$NO_2C_6H_4$	Ph	**7c**	3/81	3/85
4	4-$NO_2C_6H_4$	Ph	**7d**	3/79	3/83
5	4-$MeOC_6H_4$	Ph	**7e**	1.5/88	1.5/90
6	4-ClC_6H_4	Ph	**7f**	2.5/88	2.5/93
7	4-BrC_6H_4	Ph	**7g**	2.5/80	2.5/87
8	Ph	4-MeC_6H_4	**7h**	1.5/84	1.5/88
9	4-MeC_6H_4	4-MeC_6H_4	**7i**	1/89	1/94
10	4-ClC_6H_4	4-MeC_6H_4	**7j**	2/79	2/85
11	2-ClC_6H_4	4-MeC_6H_4	**7k**	2/84	2/86
12	3-$NO_2C_6H_4$	4-MeC_6H_4	**7l**	3/87	3/90
13	4-$MeOC_6H_4$	4-MeC_6H_4	**7m**	1/90	1/92
14	2-ClC_6H_4	4-$MeOC_6H_4$	**7n**	2.5/90	2.5/88
15	4-$NO_2C_6H_4$	4-$MeOC_6H_4$	**7o**	3/85	3/88
16	3-$NO_2C_6H_4$	4-$MeOC_6H_4$	**7p**	3.5/86	3.5/89
17	2-MeC_6H_4	4-$MeOC_6H_4$	**7q**	1/89	1/94
18	4-$MeOC_6H_4$	4-$MeOC_6H_4$	**7r**	1/96	1/93
19	4-MeC_6H_4	4-$MeOC_6H_4$	**7s**	1/79	1/84
20	Ph	4-$MeOC_6H_4$	**7t**	1.5/82	1.5/86
21	Ph	3-MeC_6H_4	**7u**	1.5/90	1.5/94
22	Ph	3-$NO_2C_6H_4$	**7v**	3/81	3/76
23	Ph	4-$NO_2C_6H_4$	**7w**	3/74	3/75
24	Ph	3-$MeOC_6H_4$	**7x**	2/90	2/79
25	Ph	4-ClC_6H_4	**7y**	3/88	3/80

Method A: DMF, reflux; Method B: US, DMF, 100 °C

Amines substituted with electron-donating groups have more reactivity when compared with those substituted with electron-withdrawing groups.

At last, we demonstrate that the catalyst could be recovered from the reaction mixture by an external magnet. The catalyst was tested for five runs without a significant decrease on the reactivity (Fig. 4).

Supplementary data summary

Details of the experimental procedures, characterization data for compounds ^{1}HNMR, ^{13}CNMR, and elemental analysis of selected compounds have been provided in the Supplementary Data file.

Acknowledgements We gratefully acknowledge financial support from the Research Council of the Velayat University.

References

1. G. Aridoss, S. Amirthaganesan, M.S. Kim, J.T. Kim, Y.T. Jeong, Eur. J. Med. Chem. **44**, 4199 (2009)
2. L.R. Pessoa de Siqueira, P.A. Teixeira de Moraes Gomes, L. Pelágia de Lima Ferreira, M.J. Barreto de Melo Rêgo, A.C. Lima Leite, Eur. J. Med. Chem. **17015**, 237 (2019)
3. S.K. Manjal, R. Kaur, R. Bhatia, K. Kumar, V. Singh, R. Shankar, R. Kaur, R.K., Bioorg. Chem. **75**, 406 (2017)
4. A.K. Jain, A. Vaidya, V. Ravichandran, S.K. Kashaw, R.K. Agrawal, Bioorg. Med. Chem. **20**, 3378 (2012)
5. M. Ghashang, H. Taghrir, M.N. Biregan, N. Heydari, F. Azimi, J. Sulfur Chem. **37**, 61 (2016)
6. H. Taghrir, M. Ghashang, Synth. React. Inorg. Met. Org. Chem. **46**, 246 (2016)
7. Z. Golestaneh, M. Ghashang, Tetrahedron Lett. **60**, 151194 (2019)
8. M.A. Ansari, D. Yadav, M. Shankar Singh, J. Org. Chem. **85**, 8320 (2020)
9. J. Luo, Z. Zhong, H. Ji, J. Chen, J. Zhao, F. Zhang, J. Sulfur Chem. **37**, 438 (2016)
10. J. Safaei-Ghomi, M. Navvab, H. Shahbazi-Alavi, Ultrason. Sonochem. **31**, 102 (2016)
11. H.-X. Pang, Y.-H. Hui, K. Fan, X.-J. Xing, Y. Wu, J.-H. Yang, W. Shi, Z.-F. Xie, Chin. Chem. Lett. **27**, 335 (2016)
12. M.P. Thakare, R. Shaikh, D. Tayade, RSC Adv. **6**, 28619 (2016)
13. N. Azgomi, M. Mokhtary, J. Mol. Catal. A Chem. **398**, 58 (2015)
14. S. David Jackson, J.S.J. Hargreaves, *Metal Oxide Catalysis* (Wiley-VCH Verlag GmbH & Co. KGaA, London, 2008)
15. J.C. Vedrine, G. Korotcenkov, *Metal Oxides in Heterogeneous Catalysis*, 1st edn. (Elsevier, Amsterdam, 2018)
16. H. Abbasi-Dehnavi, M. Ghashang, Heterocyclic Commun. **24**, 19 (2018)
17. F. Ghayour, M.R.M. Shafiee, M. Ghashang, Main Group Metal Chem. **41**, 21 (2018)
18. M. Ghashang, P. Khosravian, H. Ghayoor, Rec. Patents Nanotechnol. **11**, 154 (2017)
19. A.A. Oladipo, A.O. Ifebajo, M. Gazi, Appl. Catal. B Environ. **243**, 243 (2019)
20. Y. Liu, N. Cherkasov, P. Gao, J. Fernández, M.R. Lees, E.V. Rebrov, J. Catal. **355**, 120 (2017)
21. S. Nagai, K. Ueda, J. Ohyama, A. Satsuma, Catal. Today **303**, 40 (2018)
22. H. Eshghi, A. Javid, A. Khojastehnezhad, F. Moeinpour, F.F. Bamoharram, M. Bakavoli, M. Mirzaei, Chin. J. Catal. **36**, 299 (2015)
23. J. Miki, M. Asanuma, Y. Tachibana, T. Shikada, J. Catal. **151**, 323 (1995)
24. E. Akbarzadeh, M.R. Gholami, Res. Chem. Intermed. **43**, 5829 (2017)
25. F. Mirhashemi, M.A. Amrollahi, Res. Chem. Intermed. **45**, 2549 (2019)
26. S. Zhao, H. Jin, Y. Yang, J. Cui, Res. Chem. Intermed. **46**, 4579 (2020)
27. N. Orooji, A. Takdastan, R. Jalilzadeh Yengejeh, S. Jorfi, A.H. Davami, Res. Chem. Intermed. **46**, 2833 (2020)
28. A. Baziar, M. Ghashang, React. Kinet. Mech. Catal. **118**, 463 (2016)
29. P. Liu, S. Gao, C. Chen, F. Zhou, Z. Meng, Y. Huang, Y. Wang, Carbon **169**, 276 (2020)
30. P. Liu, Y. Zhang, J. Yan, Y. Huang, L. Xia, Z. Guang, Chem. Eng. J. **368**, 285 (2019)